Stepwise Collapse of Cyclolinear Polysiloxane Langmuir Monolayers Studied by Brewster Angle Microscopy and Grazing Incidence X-ray Diffraction

ARTICLE *in* MACROMOLECULES · MAY 2004

Impact Factor: 5.8 · DOI: 10.1021/ma049631u

7 AUTHORS, INCLUDING:

Jaime Ruiz-Garcia
Universidad Autónoma de San Luis Potosí
65 PUBLICATIONS **984** CITATIONS
SEE PROFILE

Helmuth Moehwald
Max Planck Institute of Colloids and Interfaces
1,004 PUBLICATIONS **38,672** CITATIONS
SEE PROFILE

Torben Rene Jensen
Aarhus University
247 PUBLICATIONS **4,645** CITATIONS
SEE PROFILE

N. N. Makarova
Russian Academy of Sciences
142 PUBLICATIONS **472** CITATIONS
SEE PROFILE

Stepwise Collapse of Cyclolinear Polysiloxane Langmuir Monolayers Studied by Brewster Angle Microscopy and Grazing Incidence X-ray Diffraction

Yu. K. Godovsky,*,† G. Brezesinski,*,‡ J. Ruiz-Garcia,‡,§ H. Möhwald,‡ T. R. Jensen,∥,◇ K. Kjaer,∥,⊥ and N. N. Makarova#

Karpov Institute of Physical Chemistry, Vorontsovo Pole str.10, Moscow 105064, Russia, Max-Planck Institute of Colloids and Interfaces, Am Mühlenberg 1, D-14476 Golm/Potsdam, Germany, Condensed Matter Physics and Chemistry Department and Materials Research Department, Risø National Laboratory, DK-4000 Roskilde, Denmark, Interdisciplinary Nanoscience Center, Department of Chemistry, University of Aarhus, DK-8000 Århus C, Denmark, and Nesmeyanov Institute of Elementoorganic Compounds, Russian Academy of Sciences, Vavilova str. 28, Moscow 117813, Russia

Received February 24, 2004; Revised Manuscript Received April 21, 2004

ABSTRACT: The surface-pressure-induced layering transition of a 2D nematic-like cyclolinear polyorganosiloxane that consists of six-membered rings of silicon and oxygen joined by oxygen bridges and that has phenyl side groups (CL-PMPhSi) is observed and characterized by film balance measurements, Brewster angle microscopy (BAM), and grazing incidence X-ray diffraction (GIXD) at the air/water interface. In the uncompressed state, $A \leq 95$ Å^2/monomer and $\pi \approx 0$, BAM images demonstrate partial surface coverage by solidlike birefringent islands, supporting the previously suggested model of extended aligned polymer chains lying parallel to the water surface in a quasi-two-dimensional "nematic-like" liquid-crystalline arrangement. Further compression, $A \leq 95$ Å^2/monomer, leads to a complete and uniform monolayer coverage of the surface followed by layer-by layer growth visible as stepwise increasing surface pressure. GIXD reveal one diffraction peak for monolayer as well as multilayer samples of CL-PMPhSi with a *d*-spacing of $d = (10.5 \pm 0.1)$ Å. The maximum Bragg rod intensity is observed at $q_z \approx 0$ for the monolayer but moved to a well-defined nonzero q_z value for the multilayer samples. We infer that there are planes in the structure of the CL-PMPhSi multilayers tilted by ca. 27° from the surface normal. For both mono- and multilayers, the analysis of the observed GIXD peak widths indicates that the extent of the lateral positional correlation between parallel chains ranges from about 12 for the monolayer to about 30 interchain distances in multilayers, implying some mesoscale order similar to a quasi-long-range order. Analysis of the Bragg rods allowed us to estimate the thickness of the monolayer and multilayers. Comparison of the data with independent results of molecular modeling, X-ray reflectivity, and atomic force microscopy gave very good agreement. As a result of the analysis we conclude that both in-plane and out-of-plane GIXD data reveal a high degree of stable structural order of the CL-PMPhSi films.

Introduction

Amphiphilic molecules with low molecular weight, such as fatty acids and phospholipids, readily form monomolecular films (Langmuir monolayers, LM) at the air/water interface. There has been a plethora of thermodynamic and structural studies of these monolayer systems in the past decades.[1] The two-dimensional LM formed by these amphiphiles show a rich phase behavior where up to 10 phases, which are two-dimensional analogues of gas, liquid, liquid-crystalline, and crystalline phases, have been proposed to exist.[1−6] Phase transitions between these phases can be observed by varying the temperature and/or surface pressure. If the LM is overcompressed above the equilibrium spreading pressure (ESP), at which the 2D and 3D phases coexist, it can undergo a transition to a three-dimensional state; this process is known as collapse.[7,8] Two general scenarios for the collapse are observed: a direct transition from the LM to a bulk phase or a progressive transition through a series of multilayers. In saturated fatty acids and esters, there is evidence for both the formation of multilayers and nucleation of the three-dimensional phase.[3,10−18] There is convincing evidence that smectic liquid crystals, which have a layered structure in the bulk, always form stable multilayers before complete collapse to a three-dimensional phase.[19−27] Direct observation of multilayer formation resulting from the collapse of LM has been observed by Brewster angle microscopy (BAM),[10,11] and collapsed crystallites have been analyzed by grazing incidence X-ray diffraction (GIXD)[12] and atomic force microscopy (AFM).[10−12]

Amphiphilic polymers can form stable monomolecular films at the air/water interface, and many surface-pressure−surface-area isotherm studies of polymeric LM's have been reported.[7,28,29] When the polymeric LM's are compressed above the ESP, they also undergo a transition to the bulk phase, i.e., collapse, either directly, or via stepwise formation of multilayers. The second scenario of collapse of polymeric monolayers is especially intriguing because macromolecules, which are much longer than conventional amphiphilic molecules, should lie flat on the surface rather than stand with their long axes normal to the air/water interface as do

* To whom correspondence should be addressed. E-mail: godovsky@cc.nifhi.ac.ru, brezesinski@mpikg-golm.mpg.de.
† Karpov Institute of Physical Chemistry.
‡ Max-Planck Institute of Colloids and Interfaces.
§ Permanent address: Instituto de Física, Universidad Autónoma de San Luis Potosi, Alvaro Obregón 64, S.L.P. 78000, México.
∥ Condensed Matter Physics and Chemistry Department, Risø National Laboratory.
◇ University of Aarhus.
⊥ Materials Research Department, Risø National Laboratory.
Russian Academy of Sciences.

10.1021/ma049631u CCC: $27.50
Published on Web 05/26/2004

the (much shorter) common amphiphiles. Formation of bilayers has been observed during the collapse of LM's of rodlike polypeptides in α-helical conformation.[30−33] Using BAM, specular X-ray reflectivity (XR), and GIXD, Pershan and collaborators[33] recently performed direct microscopic characterization of the first-order monolayer−bilayer transition in poly(γ-benzyl-L-glutamate) and deduced the in-plane arrangements of these rodlike macromolecules both in the monolayer and bilayer. Zhu et al.[34] observed two well-pronounced kinks in pressure−area isotherms before the collapse point in side-chain liquid-crystalline (smectic) polysiloxanes and interpreted them as monolayer phase transitions between different molecular conformations. They emphasized the role of the hydrophilic siloxane backbone (anchored on the water surface) and mesogenic side chains. For similar side-chain smectic polysiloxanes, Duran et al.[35,36] have shown that they may escape into the third dimension in a regular way under lateral compression forming bi- and trilayers at the air/water interface (similar to low molecular weight smectics).

Monomolecular layers of linear poly(dimethylsiloxane) (PDMS) have been investigated in situ at the air/water interface by several techniques, and evidence for a collapse through coiling of the polymer chains into helices was found.[29,37−40] Surface-pressure−surface-area isotherm data for PDMS show a small reversible second step after the LM formation due to coiling of the polymer chains into helices oriented with the long axis parallel to the surface. Fluorescence microscopy and external IR spectroscopy showed that in the region of high surface concentration the oxygen atoms in PDMS avoid contact with the water surface; this result suggests the formation of helices. BAM images of collapsing PDMS revealed domains of different discrete thickness and suggested collapse involving multilayer formation. However, Granick et al.[41] found similar isotherms for cyclic dimethylsiloxanes and suggest a similar mechanism of collapse, although it can be argued that helix formation in small-size cyclic siloxanes is unlikely.

During the past decade it has been recognized that linear poly(di-*n*-alkylsiloxane)s and cyclolinear polyorganosiloxanes (CL-POSi), which do not contain any mesogenic fragment neither in the main chains nor in the side chains, can form columnar and 2D nematic-like mesophases in bulk.[42−44] Despite their flexibility, these polysiloxane macromolecules have an extended chain conformation in the mesomorphic states. Moreover, many of these polysiloxanes of new macromolecular architecture can be spread as LM's on the liquid/air interface, demonstrating stepwise collapse of the monolayers during compression. Godovsky et al.[39,45−49] found up to seven plateaus in pressure−area isotherms of CL-POSi of various molecular structure. The plateaus occur at ratios of surface area consistent with stepwise layer growth from monolayer to bilayer, bilayer to trilayer, etc., continuing up to seven layers. This is clear evidence of successive multilayer transitions in a material that does not have a bulk smectic liquid-crystal phase. The stepwise collapse studied in a thin polymer film by AFM[45,47,49] showed nucleation of three-dimensional islands, which then appear to spread in the form of ribbons 0.5 μm wide and 7.5 Å high, initiating the growth of the second layer as the film is further compressed. However, this nucleation process was not observed in the higher-pressure collapse plateaus. Similar multistep collapse of LM's of flexible mesomorphic (nonmesogenic) linear poly(di-*n*-alkylsiloxane)s on the surface of H_2O/glycerine mixture was recently established.[43,50]

Although it has been proposed that the collapse plateau regions can be seen as coexistence regions between an *n*-layer and (*n* + 1)-layer (where *n* = 1, 2, 3, etc.) for CL-POSi's, nevertheless, no insight into the packing of the polymer chains was suggested until now. Here we present the first structural investigation of CL-POSi performed in situ directly at the air−water interface by means of synchrotron grazing incidence X-ray diffraction giving Angstrom-scale information. We focus on the structure and collapse process of CL-POSi in order to gain knowledge on the organization of the polymer LM's and the mechanism for their collapse to multilayer samples consisting of a well-defined number of layers. Brewster angle microscopy (BAM) is used for characterization of the morphology of monolayers and collapsed films.

Experimental Section

Polymer. We studied one of cyclolinear polyorganosiloxanes CL-POSi's with the chemical structure shown below (CL-PMPhSi). The repeating unit of the polymers is a 12-membered ring that consists of alternating silicon and oxygen atoms with an extra oxygen atom acting as a linker between the rings in the polymer chain.

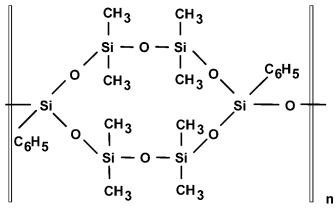

CL-PMPhSi

The phenyl groups that are connected to the silsesquioxane silicon atoms (these are the silicon atoms connected to three oxygen atoms in the polymer chain) define the polymer local tacticity. The polymer studied here is atactic CL-PMPhSi: The phenyl groups are randomly distributed along the chain.

The experimental methods to synthesize the polymers have been given in detail elsewhere.[51−55] Here, we describe briefly only the main scheme of the synthesis and the molecular characterization of monomer and polymer. The polymer was synthesized by heterofunctional polycondensation of a corresponding monomer. 2,8-Dichloro-2,8-diphenyl-4,4,6,6,10,10,-12,12-octamethylcyclohexasiloxane (**I**) and 2,8-dihydroxy-2,8-diphenyl-4,4,6,6,10,10,12,12-octamethylcyclohexa-siloxane (**II**) were prepared according to the procedure described previously but without separation of isomers.[51] The monomers **I** and **II** where characterized by X-ray diffraction and ^{1}H NMR.[56] Poly-[oxy(diphenyloctamethylcyclohexasiloxane-2,8-diyl)]s (CL-PMPhSi) was prepared according to the procedure described in ref. 51. To 1.52 g (2.50 mmol) of **I** in 3.0 mL of dry diethyl ether a solution of 1.43 g (2.50 mmol) of **II** and 0.42 g (5.0 mmol) of pyridine in 3.5 mL of dry diethyl ether was added under argon atmosphere for 0.5 h. The temperature of the reaction mixture was increased to 70 °C after addition of benzene (2.5 mL). Benzene (50 mL) was added to the reaction product, and $C_5H_5N{\cdot}HCl$ was separated off; the benzene solution was washed with water and dried under Na_2SO_4. A 1.30 g (48.0%) amount of CL-PMPhSi with an atactic structure was obtained. The characterizations of the polymers are summarized in Table 1.

Grazing Incidence X-ray Diffraction (GIXD). The X-ray scattering measurements were performed using an automatic Langmuir trough with an area of 480 cm^2 placed in an airtight aluminum container with Kapton windows. Both the trough and the moveable barrier are made of Teflon, and the surface

Table 1. Properties of the Investigated Cyclolinear Polyorganosiloxane CL-PMPhSi[a]

M_m (g/mol)	L_m (Å)	x_w	M_w (g/mol)	L_p Å	T_g (°C)	T_i (°C)	η (dl/g)	M_w/M_n
554	10.2	135	$7.5\cdot10^4$	$1.36\cdot10^3$	−40	>400	0.49	2.05

[a] Molecular weight of the monomer, M_m; length of the monomer estimated using Stuart models, L_m; average degree of polymerization given as the number of monomers per polymer, x_w; molecular weight of the polymer, M_w; contour length of the polymer, L_p; glass-transition temperature, T_g; isotropization temperature, T_i; viscosity, η; molecular weight distribution, M_w/M_n.

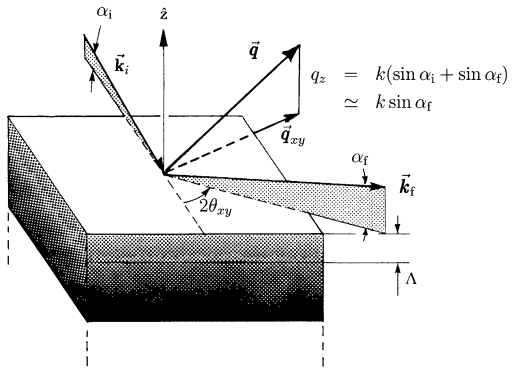

GIXD:

$$q_{xy} = k\sqrt{\cos^2\alpha_i + \cos^2\alpha_f - 2\cos\alpha_i\cos\alpha_f\cdot\cos 2\theta_{xy}}$$
$$\simeq k\sqrt{1 + \cos^2\alpha_f - 2\cos\alpha_f\cdot\cos 2\theta_{xy}}$$
$$\simeq 2k\cdot\sin(\tfrac{1}{2}\cdot 2\theta_{xy}) + \mathrm{Order}(\alpha_f^2)$$
$$q_z = k(\sin\alpha_i + \sin\alpha_f)$$
$$\simeq k\sin\alpha_f$$

Figure 1. Experimental geometry for the GIXD data collection.

pressure π is measured with a Wilhelmy filter paper plate (accuracy ±0.2 mN/m). This Langmuir trough allows variation of subphase temperature and area per molecule in the surface film during the X-ray scattering experiments. A polished glass block in the trough reduced the depth of the liquid subphase to 0.3 mm in the X-ray footprint region and thereby suppressed mechanically excited capillary waves. The liquid subphase was ultrapure water filtered in a Milli-Q apparatus (Millipore, Bedford, MA) giving a pH value of ca. 5.9 and heated to $T = (22.0 \pm 0.2)$ °C. X-ray experiments were performed in a water-vapor-saturated He atmosphere.

Monolayers were prepared by spreading a chloroform solution (spectroscopic grade) of CL-PMPhSi with a microsyringe onto water. The CL-PMPhSi concentration in the spreading solution ranged from 0.2 to 0.7 mg/mL, and the volume of the solution spread ranged from 50 to 150 μL. No systematic dependence of monolayer quality on the concentration and the spreading volume was observed in this study. After evaporation of the solvent, the film was compressed to an area corresponding to monolayer formation, which has been estimated using previous results.[45−49] After the film was slowly compressed to a desired area/monomer, A, which was preselected using $\pi-A$ isotherms obtained in previous investigations, the compression was stopped and the constant pressure regime was maintained. During all the X-ray measurements at the target pressure the mono- and multilayers were stable for at least several hours and no detectable radiation damage or other transformations of the films was observed.

GIXD experiments were performed at the undulator beam line BW1[57] at the synchrotron radiation facility HASYLAB at DESY (Hamburg, Germany). A monochromatic X-ray beam, $\lambda = 1.304$ Å, was selected with a Be(002) monochromator crystal. The experimental geometry for the data collection is illustrated in Figure 1. The incident grazing angle α_i of the X-ray beam was $\sim 0.85\alpha_c$, where $\alpha_c = 0.129°$ is the critical angle for total external reflection from an air/water interface. This limits the penetration depth of the beam to 5−10 nm.[58] Thus, X-ray scattering from the water subphase contributing to the background intensity is efficiently reduced allowing accurate measurements of the X-ray photons diffracted from the liquid-crystalline monolayer. There is evidence (see later) that the sample is composed of a large number of liquid-crystalline domains consisting of presumably extended-chain macromolecules laying flat on the water surface in such a way that siloxane fragments adjoin to the water, while the majority of hydrocarbon side groups are directed toward the air. The solidlike domains are randomly oriented on the water surface with respect to the orientation of the macromolecules in the domains, resembling a 2D powder. The dimension of the X-ray footprint on the sample was ~2−50 mm².[58]

The diffracted X-rays were detected by a position-sensitive detector covering approximately $0 < \alpha_f < 15°$ and scanned along the $2\theta_{xy}$ arc in the range $1° < 2\theta_{xy} < 40°$. The angle between the horizontal plane and the diffracted beam is denoted α_f, and the angle between the incident and diffracted beam projected onto the horizontal plane is $2\theta_{xy}$. The scattering vector $\boldsymbol{q}$ can be decomposed to $\boldsymbol{q} = \boldsymbol{q}_{xy} + \boldsymbol{q}_z$, and these two components are given by[59,60]

$$q_z = k\,[\sin(\alpha_i) + \sin(\alpha_f)] \approx k\,\sin(\alpha_f) \quad (1)$$

$$q_{xy} = k\,[\cos^2(\alpha_i) + \cos^2(\alpha_f) - 2\cos(\alpha_i)\cos(\alpha_f)\cos(2\theta_{xy})]^{1/2} \approx 2k\,\sin(2\theta_{xy}/2) \quad (2)$$

where the wave vector $k = 2\pi/\lambda$. Thus, the measured GIXD data can be visualized as contour plots with the intensity shown as a function of q_{xy} and q_z or projected onto the q_{xy} or q_z axes as Bragg peak or Bragg rod data, respectively. The lattice spacing d_{hk} can be obtained from the in-plane diffraction data, i.e., the position of maximum Bragg peak intensity, ${q_{xy}}^{hk}$

$$d_{hk} = 2\pi/{q_{xy}}^{hk} \quad (3)$$

where the Bragg peaks have been indexed by the Miller indices h,k to yield the unit cell parameters for the in-plane lattice.[58−60] In the case of a rectangular unit cell, the lattice parameters a and b can be calculated from d_{hk}

$$1/{d^2}_{hk} = h^2/a^2 + k^2/b^2 \quad (4)$$

The full-width at half-maximum (fwhm) of the Bragg peaks, Δq_{xy}, yields the in-plane correlation length, $L_{xy} \approx (0.88\cdot 2\pi)/\Delta q_{xy}$. The fwhm of the Bragg rods, Δq_z, gives a first estimate of the film thickness: $h_z \approx (0.88\cdot 2\pi)/\Delta q_z$.[60]

Brewster Angle Microscopy (BAM). The BAM setup used in this study has been described previously.[23,61] The BAM (BAM 1, NFT Goettingen, Germany) was mounted on the Langmuir film balance with an area of 1000 cm². The light source for the BAM was a He−Ne laser (10 mW); after p-polarization the beam is directed onto the aqueous subphase under the Brewster angle. The lateral resolution of the instrument is about 4 μm. The BAM images presented here are mirror images, since the reflected beam is directed into the CCD camera by a mirror. The BAM images were corrected for geometric distortion due to the observation at the Brewster angle (53.1°). In the present paper, a large part (400 × 400 μm²) of the original images was used.

Results and Discussion

Surface-Pressure−Area ($\pi-A$) Isotherms. Extensive isotherm studies of CL-POSi's are described elsewhere,[39,40,45,46,48,49] and only results concerning CL-PMPhSi are briefly reviewed here in order to place our measurement with the liquid surface X-ray diffractometer in context. The isotherms measured here are consistent with previous studies, and an example is shown in Figure 2. At large values of area per monomer

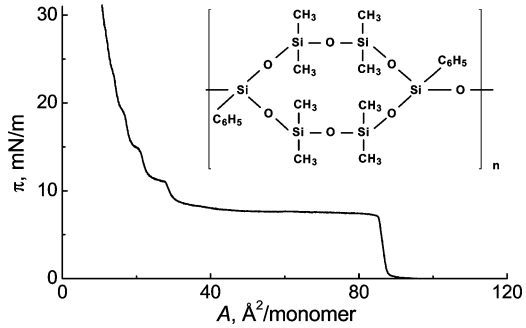

Figure 2. $\pi-A$ isotherm for CL-PMPhSi at 22 °C. Compression rate is 5 Å^2/(monomer × min).

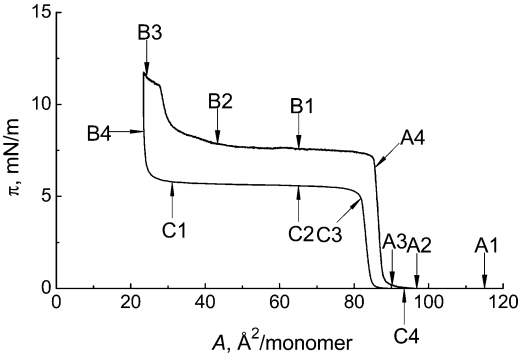

Figure 3. $\pi-A$ isotherm for CL-PMPhSi at 22 °C. Arrows indicate the points where the BAM images have been taken (see Figure 4).

A (A > 100 Å^2/monomer), the surface pressure remains at $\pi \approx 0$ (immeasurably low) as the film is compressed.

The surface pressure π increases almost linearly after completion of a monolayer, previously estimated to 93 Å^2, and reaches a plateau at approximately 85 Å^2.[46] Such a behavior is typical for molecules which have a strong tendency to self-aggregation into solidlike domains and cover the surface at large areas only incompletely. From a thermodynamic point of view, at zero surface pressure a condensed phase (the solidlike domains of extended macromolecules) and a gas-analogous phase (very diluted solution of macromolecules, which may be coiled) are in coexistence. In the following part of the paper the very diluted gas-analogous phase will be referred to as bare water surface. Hence, at A > 100 Å^2/monomer, compression is accompanied only by a reduction in the area of the gaps between the solidlike domains. This initial shape of the CL-PMPhSi isotherm resembles also the stress−strain behavior of plastics. In general, further compression leads to several steps and plateaus in the surface pressure at approximately 1/2, 1/3, ..., 1/n of the monolayer area corresponding to the formation of a film with n layers (n = 2−6). In contrast to the cyclolinear polysiloxanes with methyl substituents, in which all the steps in the isotherm data are well pronounced,[39,45] the second step for CL-PMPhSi is less pronounced at room temperature and above (Figure 2). However, at lower temperatures the second step in the isotherm for CL-PMPhSi is clearly visible at an area per repeating unit of about 46 Å^2 corresponding to the transformation of the bilayer to a trilayer.[46−48]

The pressure of the first plateau is approximately 7.5 mN/m, which is close to the ESP for CL-PMPhSi (6.7 mN/m),[49] suggesting a monolayer−bilayer coexistence regime being close to the equilibrium state. At constant area, relaxation of the surface pressure can be observed at the second or higher plateaus showing that the higher plateaus are nonequilibrium states.[39,46−48] It is important to emphasize that thin films of CL-PMPhSi were found to be stable for hours, allowing several GIXD and XR experiments to be performed on each sample (an GIXD and XR investigation takes approximately 90 min). Therefore, for practical purposes the thin films of CL-PMPhSi are considered to be stable structures. Notice, however, the isotherms are measured during continuous compression of the sample in contrast to X-ray experiments, GIXD presented here and XR,[63] which are performed at constant surface pressure of the sample.

In the first plateau the compressibility is infinite ($\chi = -A^{-1}\, dA/d\pi = \infty$), which indicates a first-order phase transition between two coexisting phases: the monolayer and bilayer.[46] The behavior at the higher plateaus cannot directly be treated in a similar manner because the higher plateaus are in nonequilibrium states and the surface pressure contains, besides the thermodynamic contribution, a dynamic (rheological) contribution.

Brewster Angle Microscopy (BAM) Images. Detailed information on the macroscopic film morphology and lateral heterogeneity is obtained by BAM according to the $\pi-A$ isotherm in compression−decompression mode (Figure 3). The BAM images obtained at low density (Figure 4) clearly indicate macroscopic heterogeneity of the surface after the deposition of the polymer solution. As it is seen from the image (A1), the surface at $A \approx$ 115 Å^2/monomer includes both regions covered with the LM and bare water areas (areas of dilute solution of macromolecules). Moreover, such LM-covered regions themselves consist of a network of monolayer islands (seen as bright areas) with gaps of bare water surface of various dimensions in between (seen as dark areas). Investigation of the birefringence effects by using an analyzing polarizer placed after the imaging lens clearly showed optical anisotropy of the network of monolayer islands. The contrast in the texture changes with the orientation of the analyzer, which seems to be associated with molecular anisotropy and indicates the existence of quasi-long-range orientation order within the regions. The structural picture emerging from the image (A1) agrees, in general, with previous BAM observations of CL-PMPhSi.[49] The existence of optical anisotropy also supports the suggestion of a "nematic-like" structure of the domains (islands) forming the network floating on the water surface. The optical anisotropy of the islands (not visible in this BAM picture) and the shape of their boundaries, which would not be expected for fluidlike islands, indicate the solidlike nature of the domains (islands). On further compression (images A2 and A3) the continuity of the monolayer network extends considerably due to complete coalescence of all islands while bare water areas at first became smaller and finally are seen only as separate holes of various sizes inside the monolayer. At this stage the surface pressure is still immeasurably low ($\pi \approx 0$) during compression.

The onset of a measurable surface pressure corresponds to the point at which practically all holes inside the monolayer have disappeared. Starting from this value of the area per monomer, A, the monolayer can sustain the surface pressure π. On further compression, when the surface pressure π begins to increase linearly with decreasing A, the whole surface is covered with the LM of CL-PMPhSi. This is well documented in the

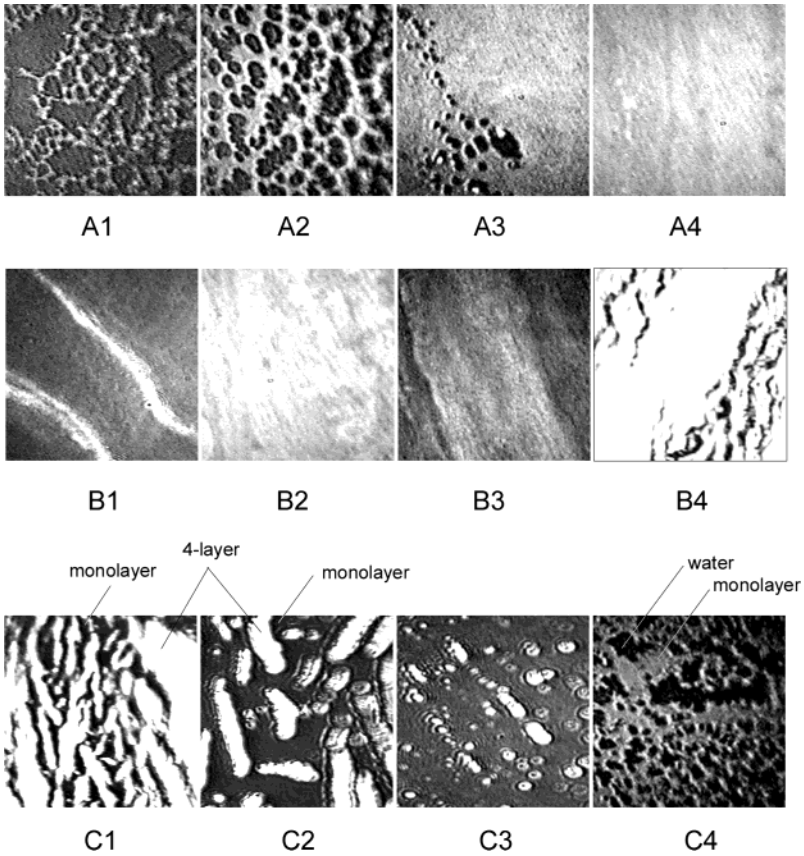

Figure 4. BAM images taken at various values of A (Å^2/monomer) indicated in the isotherm with arrows (see Figure 3): (A) A1 ~115 ($\pi \approx 0$), A2 ~97 ($\pi \approx 0$), A3 ~92 ($\pi \approx 0$), A4 ~86 ($\pi \approx 6.6$ mN/m); (B) B1 ~65 ($\pi \approx 7.5$ mN/m), B2 ~43 ($\pi \approx 8.0$ mN/m), B3 ~24 ($\pi \approx 11.5$ mN/m), B4 ~23.5 ($\pi \approx 8.5$ mN/m); (C) C1 ~31 ($\pi \approx 5.7$ mN/m), C2 ~65 ($\pi \approx 5.5$ mN/m), C3 ~82 ($\pi \approx 4.8$ mN/m), C4 ~93 ($\pi \approx 0$). Image sizes are ~400 × 400 μm^2.

image (A4) taken at the very end of the linear increase of π. As it is seen from the BAM image, just before the beginning of the first plateau the monolayer surface looks rather homogeneous.

In the first coexisting plateau region the second layer appears in the form of wide bands up to about 1 mm in length and 10−30 μm wide (B1). The density of bands increases as the film is compressed until the entire surface is covered by the bilayer, image B2. The formation of a trilayer and thicker multilayers can be observed upon further compression. The surface morphology on the third and further plateaus during collapse is less pronounced due to a lower contrast (image B3); however, at the end of every plateau the surfaces of the multilayers are rather homogeneous (for example, bright part of the image B4). BAM images (C1−C4) obtained during decompression of the film formed at the end of the third plateau (according to the isotherm it corresponds to the formation of 4-layers films, which also supports by XR measurements[63]) show that the surface layer fractures into islands of multilayers separated by the monolayer. The number of islands decreases with decompression until only LM remains floating on the water surface. Further decompression is accompanied by appearance of small holes in the LM and the surface morphology starts to resemble the initial state (image A1). The BAM images obtained for various stages along the CL-PMPhSi $\pi-A$ isotherm agree, in general, with the previously obtained less detailed BAM investigation.[46]

Grazing Incidence X-ray Diffraction (GIXD) Measurements. The bulk mesomorphic state of CL-POSi's with six-membered rings in the macromolecules can be identified as a quasi 2D nematic liquid-crystalline system with conformationally disordered polymers oriented parallel in domains.[44] The domains are randomly oriented in the bulk mesomorphic state of CL-POSi's; therefore only one X-ray diffraction peak is expected for the bulk state of these polymers, resulting from the out-of-plane periodicity.[44] According to the X-ray data for bulk CL-PMPhSi, the thickness of the sheets is (10 ± 1) Å. The periodicity in the direction normal to the macromolecular axes (interchain distance) inside the monolayerlike sheets (in plane) in the bulk state was estimated using the Stuart−Briggleb model for CL-PMPhSi, giving ~10 Å.[55]

Assuming that the monolayer and the collapsed films of CL-PMPhSi possess liquid-crystalline-like in-plane correlation, a diffraction peak corresponding to the repeating distance of the monomer unit along the polymer chain is expected. The length of the monomer unit is estimated to 10−11 Å for CL-PMPhSi.[55] However, the conformational disordering of the extended, flexible polymer chains of CL-POSi's in the bulk mesomorphic state and the atactic structure of CL-PMPhSi apparently prevent in-plane periodicity along the polymer chains.[62] Furthermore, the polymers are not necessarily in perfect registry in the direction of their long axis. Each CL-PMPhSi polymer has approximately 270 phenyl rings, suggesting that $\pi-\pi$ interaction is an important intermolecular interaction but possibly disordered due to the atactic nature of the polymer. Below we compare the X-ray characteristics of the bulk state of CL-PMPhSi with the GIXD results.

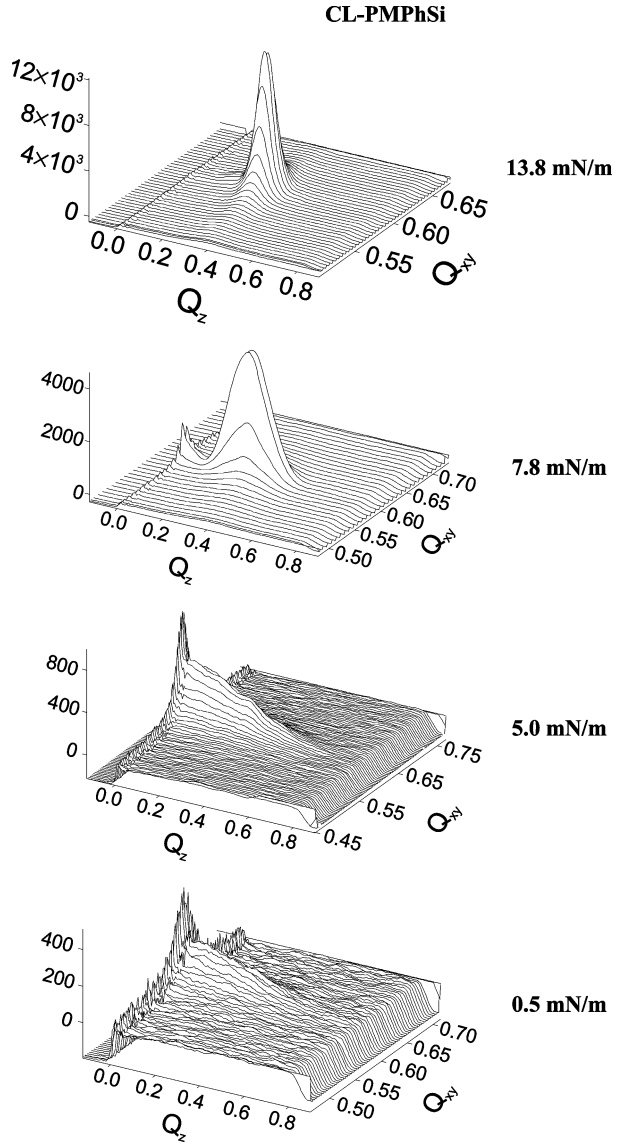

Figure 5. GIXD patterns of CL-PMPhSi at the air/water interface at various surface pressures (indicated) along the isotherm.

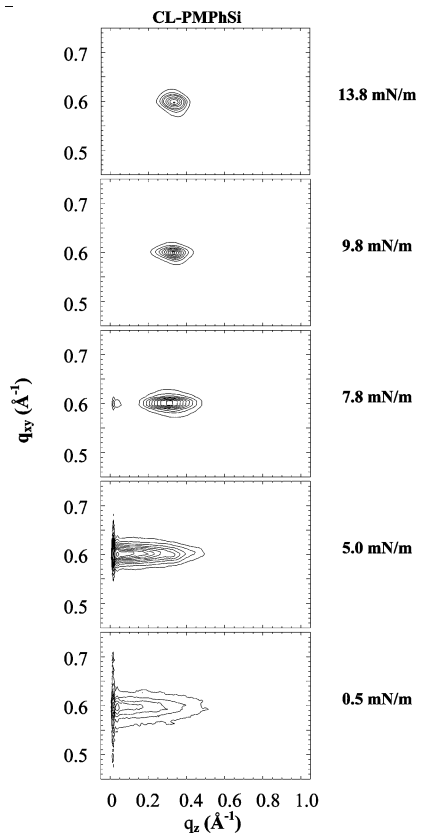

Figure 6. Contour plots of the diffracted intensity as a function of the in-plane and out-of-plane scattering vector components q_{xy} and q_z, respectively, at different surface pressures (indicated) along the isotherm.

Selected GIXD data for thin films of CL-PMPhSi are shown in Figures 5 and 6 as 3D surface and 2D contour plots. The data demonstrate that scattering from the monolayer and the collapsed films of this polymer shows only one Bragg peak, as suggested above. The Bragg peaks were fitted by Lorentzians with linear background terms, while Bragg rods were fitted by Gaussian curves, and examples of best fits are shown as solid lines in Figures 7 and 8. The GIXD data show that the maximum of the Bragg peak is at $q_{xy} \approx 0.60$ Å^{-1} independent of the surface pressure . The corresponding lattice spacings are summarized in Table 2, which lists the GIXD data and parameters obtained from the GIXD experiments for the monolayers and the collapsed films. Table 2 shows that $d = (10.5 \pm 0.1)$ Å for both the monolayer and collapsed films. This value is in good correspondence with molecular modeling, which gives $d = 10-11$ Å.[49,55] Analysis of the observed fwhm for the Bragg peaks, Δq_{xy}, yields the in-plane correlation length, L_{xy}, i.e., the extent of lateral positional correlations within the sample, perpendicular to the macromolecules. According to Table 2, the correlation length in the relaxed monolayer is $L_{xy} \approx 145$ Å, which corresponds to about 14 interchain distances. In the compressed monolayer ($\pi \approx 5$ mN/m) the correlation length is very similar, indicating that macroscopic compression in this region does not change the packing properties. The diffraction peaks become more narrow at the first ($\pi \approx 7.2$ mN/m), second ($\pi \approx 7.8$ mN/m), and third ($\pi \approx 9.8$ mN/m) collapse plateau, indicating a larger in-plane molecular correlation of $L_{xy} \approx 230-275$ Å, corresponding to ca. 30 polymer chains.

In contrast to the Bragg peaks observed at almost the same position for all samples, the behavior of the Bragg rods (Figure 8) is more complex. At low surface pressure ($0 \leq \pi \leq 0.5$ mN/m) a relatively broad Bragg rod is observed. The fits assuming zero or nonzero q_z positions are equally good, so that a clear decision cannot be made. Table 2 shows that the estimated effective thickness of the monolayer obtained from the Bragg rod depends on the assumed q_z peak position and ranges between 7.4 and 8.8 Å. Compression of the monolayer leads to a small increase of the thickness. Hence, we can estimate the thickness of the first monolayer floating on the water surface as $h_z \approx 8.5 \pm 1$ Å.

The thickness of a CL-PMPhSi monolayer has also been measured by other techniques, e.g., after transfer on solid support (mica) by SFM. Two independent measurements yielded values of $h_z = 12 \pm 1$ and 10−12 Å, respectively.[46,49] These values of h_z are also in agreement with the layer thickness of 10.9 Å obtained from molecular modeling and 10.5 Å calculated from the area of the monolayer coverage assuming that the density of the polymer is 1 g cm^{-3}.[49] X-ray data for the bulk state of CL-PMPhSi result in a value of $h = 9.3$ Å,[44] which is in the range obtained with GIXD. Finally,

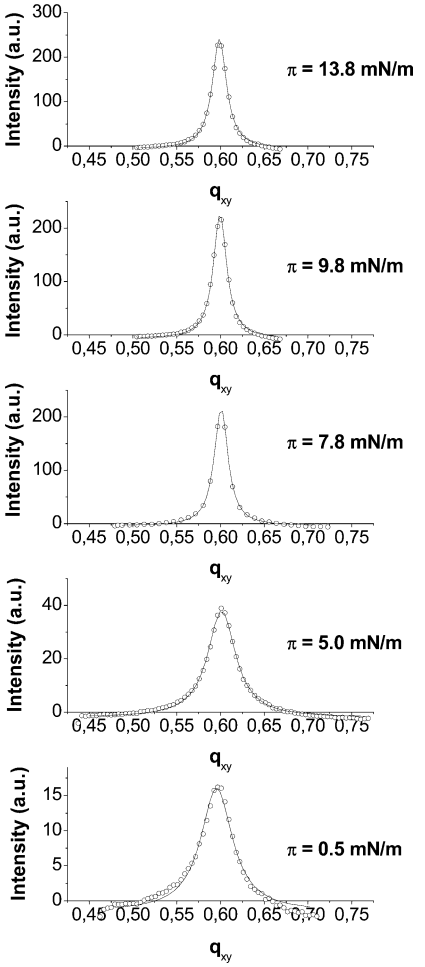

Figure 7. Bragg peaks of CL-PMPhSi monolayer and multilayer films at various surface pressures (indicated). Solid curves are best fits (Lorentzian).

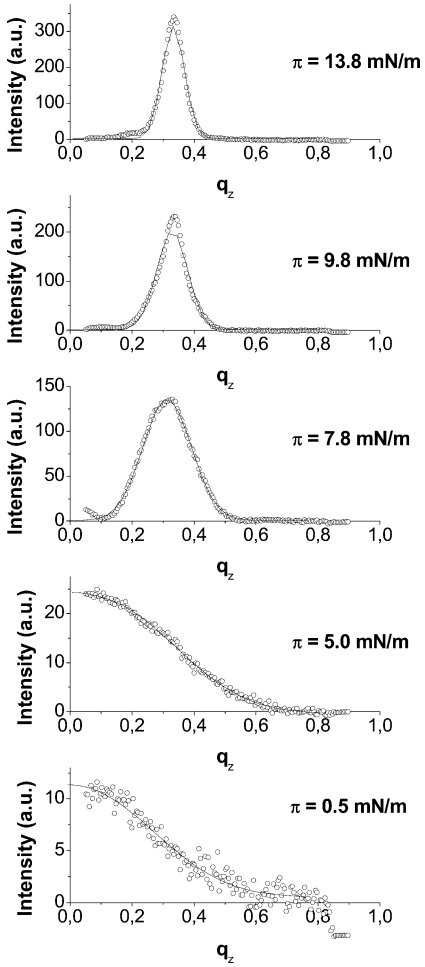

Figure 8. Bragg rods along q_z of CL-PMPhSi monolayer and multilayer films at different surface pressures (indicated). Solid lines are the best fits (Gaussian).

our recent X-ray reflectivity analysis gives $h = 10.5$ Å for the monolayer of CL-PMPhSi floating on the air/water interface.[63] The above-mentioned results suggest that the thickness of the CL-PMPhSi monolayer is 9.5 ± 1 Å. The value obtained with GIXD experiments is slightly smaller compared with the other methods. Similar behavior was observed in the investigation of three-block organosiloxane amphiphilic smectic liquid crystals at the air−water interface, in which the aromatic part of the monolayer is found to be partly immersed into water.[26]

Approximately in the middle of the first plateau ($A \approx 60$ Å^2) the estimated effective thickness is $h \approx 19$ Å, which corresponds very well to twice the value of the monolayer thickness and agrees with the monolayer−bilayer coexisting regime at the first plateau. This thickness agrees well with the layer thickness observed by XR, $L = 10.3$ Å.[63] The Bragg rod maximum moves to a nonzero q_z value for the bilayer sample corresponding to a tilt of the lattice plane; possibly the first indication of a transformation to a 2D nematic structure. At the end of the first plateau or beginning of the second step of the $\pi-A$ isotherm corresponding to the complete formation of the bilayer, the effective thickness is in the range of $h \approx (24 \pm 1)$ Å. This thickness is slightly larger than the total thickness of a bilayer observed by XR[63] and could indicate that the formation of the third layer has partially started.

Further compression leads to the formation of collapsed films with thicknesses close to three layers ($h \approx$ 32 Å) and four layers ($h \approx 40$ Å). However, different monolayers may give different thicknesses at the same surface pressure in the high-pressure region, e.g., $h =$ 41.8 and 55.4 Å observed in different experiments at $\pi = 9.8$ mN/m, corresponding to films consisting of approximately four and five monolayers, respectively. One can assume that the difference reflects the different values of the area (beginning and end of the plateau) at the same surface pressure, which is kept constant during the GIXD experiments. Finally, the highest value of surface pressure π reached in these GIXD experiments was $\pi = 13.8$ mN/m. In the continuous compression mode this value corresponds to the formation of a multilayer film with a thickness equal to 6−7 monolayers ($h \approx 60-70$ Å). However, the thickness estimated from the Bragg rod is $h \approx 80$ Å, which is slightly larger and corresponds rather to 7−8 layers in the multilayer film. Again, this may be connected with the different values of surface areas at the same surface pressure. Hence, we see that, in general, the agreement between the number of monolayers in the multilayers estimated from isotherms and Bragg rods is quite satisfactory.

Only one diffraction peak is observed in the bilayered and multilayered films of CL-PMPhSi (as for the monolayers). Both for mono- and multilayers we assume that this peak is due to the horizontal *inter*polymer stacking repeat and rationalize the absence of any further peaks (that would involve also the *intra*polymer repeat distance from one monomer to the next) as due to confor-

Table 2. Averaged GIXD Parameters Obtained for the Monolayer and Collapsed Films of CL-PMPhSi

π^a (mN/m)	d (Å)	q_{xy} (Å^{-1})	Δ_{xy} (Å^{-1})	q_z (Å^{-1})	q_z (Å^{-1})	L_{xy}/d	h_z (Å)	h_z/n^b (Å)	t^c (deg)
0.5	10.49	0.599	0.038	0	0.749	13.8	7.4	7.4	n/a
				0.064	0.626	13.8	8.8	8.8	n/a
5.0	10.44	0.602	0.038	0	0.688	13.9	8.2	8.2	n/a
				0.071	0.566	13.9	9.8	9.8	n/a
6.8	10.37	0.606	0.022	0.260	0.297	24.3	19.0	9.5	23
7.2	10.45	0.601	0.024	0.291	0.230	22.0	24.0	12.0	26
7.8	10.45	0.601	0.020	0.315	0.172	26.4	32.1	10.7	28
9.0	10.47	0.600	0.020	0.320	0.138	26.4	40.1	10.0	28
9.8	10.47	0.600	0.010	0.328	0.120	26.4	46.1	11.5	29
13.8	10.49	0.599	0.020	0.330	0.070	26.3	80	11.4	28

[a] Average values of three different experimental runs. [b] n is the number of layers corresponding to the indicated surface pressure π of the isotherm obtained in the continuous compression regime. [c] n/a = not applicable.

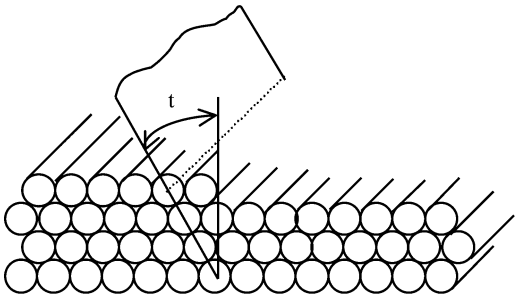

Figure 9. Schematic view of packing of macromolecules in multilayers indicating the tilt angle t.

mational disorder and/or nonregistry of one polymer along the next, as discussed above.

In contrast to the monolayers, for the multilayers the position of the Bragg rod maximum is clearly shifted to a nonzero q_z value. To explain this observation we are inspired by the analysis[1,58,59,60,65] of classical Langmuir monolayers of simple linear amphiphilic molecules where Bragg rod maxima at nonzero q_z indicate that the (all parallel) aliphatic chains are tilted and the tilt angle t from the vertical as well as the azimuthal tilt direction can be deduced from the set of equations

$$q_z^{hk} = q_{xy}^{hk} \tan(t) \cos(\psi_{hk}) \quad (5)$$

where ψ_{hk} is the angle between the horizontal projection of the tail and the scattering vector $\boldsymbol{q}_{xy}^{hk}$. Equation 5 follows from the observation that only when the scattering vector $\boldsymbol{q} = \boldsymbol{q}_{xy} + \boldsymbol{q}_z$ is in a *plane* orthogonal to the *line* defined by the long axis of the molecule will all parts of the molecule scatter in phase.[59,65]

The present case is somewhat simpler. The stacked polymers may form *planes* of high electron density, and the scattering from such a plane will add in phase only when the scattering vector $\boldsymbol{q} = \boldsymbol{q}_{xy} + \boldsymbol{q}_z$ points along a *line* orthogonal to the *plane*, so that the q_z and q_{xy} maximum positions of the observed peak must obey the single equation

$$q_z = q_{xy} \tan(t) \quad (6)$$

where t is the tilt angle of the planes (see Figure 9). Planar tilt angles (Table 2) increasing from 23° to 28° from the surface normal result on going from bilayer to multilayer films. A preliminary computer simulation, assuming an orthorhombic packing of the CL-PMPhSi, agrees with the results obtained from the experiments.

Summary and Conclusions

By BAM and GIXD we investigated monolayers and multilayers of a 2D nematic-like liquid-crystalline cyclolinear polyorganosiloxane at the air−water interface. On the basis of the results presented in this paper and obtained previously, the following model of structural changes has been deduced.

Just after being spread from a dilute solution on the water surface at large values of area A, CL-PMPhSi macromolecules lie down flat as 2D coils on water surface but immediately start to aggregate laterally aligning themselves parallel to their nearest neighbors due to the 2D nematic-like nature of their bulk state at room temperature. This aggregation is accompanied by the formation of 2D solidlike islands floating on the water surface where the macromolecules in each island are more or less extended and parallel. Compression of the floating islands on this stage has no influence on the surface pressure ($\pi = 0$) because it is accompanied by only the reduction of the liquid (bare water or very dilute solution) surface coexisting with monolayer islands without any structural changes at the intermolecular level. Indeed, as seen by BAM, neighboring islands contact each other during compression and aggregate to larger islands to form finally a net, which initially contains a lot of holes of various sizes. However, these defects gradually disappear and the monolayer homogeneously covers the entire liquid surface.

Further compression is accompanied by a steep linear rise in the surface pressure. The linear behavior of π as a function of relative molecular area is very similar to the bulk stress−strain behavior of typical polymer plastics (crystalline and glassy) as already emphasized in the literature.[64] During the steep increase of the surface pressure the macromolecules remain laying flat on the water surface and the interchain distance ($d \approx$ 10.5 Å) is independent of pressure, which the monolayer can sustain before collapse. The transition pressure to a bilayer is close to the equilibrium spreading pressure of CL-PMPhSi. The single diffraction peak at zero or close to zero q_z found for the monolayer is the result of a regular variation of electron density only in the direction normal to the axes of the macromolecules, while along the macromolecules due to conformational disorder and nonregistry the electron density is not distributed in a regular manner to give rise to diffraction. We suggest that due to this feature the monolayer can be viewed as a dense quasi-two-dimensional nematic liquid crystal confined to the water surface.

Collapse of the monolayer results initially in the first plateau of constant π in the π−A isotherm, which has previously been attributed to a first-order monolayer−bilayer phase transition.[46] Further compression is accompanied by the appearance of several steps in the surface pressure and several plateaus, correspondingly, resulting from multilayer formation. GIXD measure-

ments support the picture that the second and following (up to six) layers, which have the same horizontal interchain *d*-spacing as the monolayer, gradually cover the top surface of the bottom layer during the stepwise collapse until full coverage and beginning of formation of the next layer. The multilayered structure is stable at a constant supporting lateral pressure at least for several hours, which seems to be a direct result of the tendency of CL-PMPhSi macromolecules to aggregate into a liquid-crystalline phase. However, because of the atactic structure of the macromolecules, the system remains in the noncrystalline state up to the highest surface pressure that it can sustain. For both mono- and multilayers, analysis of the observed GIXD peak widths indicates that the extent of lateral correlations between parallel CL-PMPhSi macromolecules ranges from about a dozen (for the monolayer) to ~25 (for multilayers) interchain distances, demonstrating a mesoscale-range order for the collapsed films.

Although the surface-pressure−surface-area isotherms and GIXD experiments are performed in different modes (either at constant compression rate or at constant surface pressure, respectively), the estimated thickness of the monolayer and multilayered films using the two different methods are in a good agreement, also with other experimental results, e.g., XR,[63] molecular modeling,[49] AFM,[49] and bulk X-ray analysis of the liquid-crystalline polymer.[44] Hence, the idea that the observed plateaus in surface-pressure−area isotherms are consistent with stepwise layer growth from monolayer to bilayer, bilayer to trilayer, etc., is supported by the present GIXD experiments performed in situ at the air−water interface, providing Angstrom-scale structural information.

Acknowledgment. This work is part of the INTAS and RFBR (Russian Foundation for Basic Research) research programs supported under the grants INTAS 97-485 and RFBR 99-03-33351. We are grateful to the Danish National Research council under the DANSYNC program and the European Community (Contract HPRI-CT-1999-00040) for financial support as well as to HASYLAB at DESY, Hamburg, Germany, for beam time. Yu.K.G. thanks the Alexander von Humboldt Foundation for a Research Award. J.R.-G. acknowledges support from the Alexander von Humboldt Foundation and CONACYT. T.R.J. thanks the Danish National Research Council for a *Steno* Stipend.

References and Notes

(1) Kaganer, V. M.; Möhwald, H.; Dutta, P. *Rev. Mod. Phys.* **1999**, *71*, 779.
(2) Kaganer, V. M.; Loginov, E. B. *Phys. Rev. E* **1995**, *51*, 2237.
(3) Bibo, A. M.; Knobler, C. M.; Peterson, I. R. *J. Phys. Chem.* **1991**, *95*, 5591.
(4) Lundquist, M. *Chem. Scr.* **1971**, *1*, 5.
(5) Lundquist, M. *Chem. Scr.* **1971**, *1*, 197.
(6) Lin, B.; Shih, M. C.; Bohanon, T. M.; Ice, G. T.; Dutta, P. *Phys. Rev. Lett.* **1990**, *65*, 191.
(7) Gaines, G. L. *Insoluble monolayers at Liquid−Gas Interfaces*; Interscience: New York, 1966.
(8) Smith, R. D.; Berg, J. C. *J. Colloid Interface Sci.* **1980**, *74*, 273.
(9) Bommarito, G. M.; Foster, W. J.; Pershan, P. S.; Schlossman, M. L. *J. Chem. Phys.* **1996**, *105* (12), 5265.
(10) Vollhard, D.; Kato, T.; Kawano, M. *J. Phys. Chem.* **1996**, *100*, 4141.
(11) Galvan-Miyoshi, J.; Ramos, S.; Ruiz-Garcia J.; Castillo, R. *J. Phys. Chem.* **2001**, *115*, 8178.
(12) Meine, K.; Weidemann, G.; Vollhardt, D.; Brezesinski, G.; Kondrashkina, E. A. *Langmuir* **1997**, *13*, 6577−6581.
(13) Ries, H. E. *Nature* **1979**, *281*, 287.
(14) Ries, H. E.; Walker, D. C. *J. Colloid Sci.* **1961**, *16*, 361.
(15) Richardson, R. M.; Roser, S. J. *Langmuir* **1991**, *7*, 1458.
(16) Siegel, S.; Hönig, D.; Vollhardt, D.; Möbius, D. *J. Phys. Chem.* **1992**, *96*, 8157.
(17) Vollhardt, D.; Gutberlet, T. *J. Colloids Surf.* **1995**, *102*, 257.
(18) Kato, T.; Matsumoto, N.; Kawano, M.; Suzoki, N.; Araki, T.; Irigama, K. *Thin Solid Films* **1994**, *242*, 223.
(19) Rapp, B.; Gruler, H. *Phys. Rev. A* **1990**, *42*, 2215.
(20) Xue, J. Z.; Jun, C. S.; Kim, M. W. *Phys. Rev. Lett.* **1992**, *69*, 474.
(21) Friedenberg, M. C.; Fuller, G. G.; Frank, C. W.; Robertson, C. R. *Langmuir* **1994**, *10*, 125.
(22) deMul, M. N. G.; Mann, J. A., Jr. *Langmuir* **1994**, *10*, 2311.
(23) Ibn-Elhaj, M.; Riegler, H.; Möhwald, H. *J. Phys. I* **1996**, *6*, 969.
(24) Harke, M.; Ibn-Elhaj, M.; Möhwald, H.; Motschmann, H. *Phys. Rev. E* **1998**, *57*, 1806.
(25) Ibn-Elhaj, M.; Möhwald, H.; Cherkaoui, Z.; Zniber, R. *Langmuir* **1998**, *14*, 504.
(26) Ibn-Elhaj, M.; Riegler, H.; Möhwald, H.; Schwendler, M.; Helm, C. A. *Phys. Rev. E* **1997**, *56*, 1844.
(27) Fang, J. Y.; Uphaus, R. A. *Langmuir* **1994**, *70*, 1005.
(28) Gaines, G. L., Jr. *Langmuir* **1991**, *7*, 834.
(29) Arslanov, V. V. *Russ. Chem. Rev.* **1994**, *63*, 1.
(30) Malcolm, B. R. *Polymer* **1966**, *7*, 595.
(31) Malcholm, B. R. *Proc. R. Soc. A* **1968**, *305*, 363.
(32) Takenaka, T.; Harada, K.; Matsumoto, M. *J. Colloid Interface Sci.* **1980**, *73*, 569.
(33) Fukoto, M.; Heilmann, R. K.; Pershan, P. S.; Yu, S. M.; Griffith, J. A.; Tirrell, D. A. *J. Chem. Phys.* **1999**, *111* (21), 9761.
(34) Zhu, T.-M.; Lu, Z.-H.; Wei, Y. *Phys. Rev. E.* **1994**, *49*, 5316.
(35) Fadel, H.; Percec, V.; Zheng, Q.; Adincula, R. C.; Duran, R. S. *Macromolecules* **1993**, *26*, 1650.
(36) Adams, J.; Buske, A.; Duran, R. S. *Macromolecules* **1993**, *26*, 2871.
(37) Noll, W.; Steinbach, H.; Sucker, H. *J. Polym. Sci.* **1971**, *C34*, 123.
(38) Mann, E. K.; Hennon, S.; Langevin, D.; Meunier, J. *J. Phys. II* **1992**, *2*, 1683.
(39) Belousov, S. I.; Sautter, E.; Godovsky, Yu. K.; Makarova, N. N.; Pechhold, W. *Russ. Polym. Sci.* **1996**, *A38*, 1532.
(40) Sautter, E.; Belousov, S. I.; Pechhold, W.; Makarova, N. N.; Godovsky, Yu. K. *Russ. Polym. Sci.* **1996**, *A 38*, 39.
(41) Granick, S.; Clarson, S. J.; Formoy, T. R.; Semlyen, J. A. *Polymer* **1985**, *26*, 925.
(42) Godovsky, Yu. K.; Papkov, V. S. *Adv. Polym. Sci.* **1989**, *88*, 129.
(43) Mollenberg, A.; Möller, M.; Sautter, E. *Prog. Polym. Sci.* **1997**, *22*, 1133.
(44) Godovsky, Yu. K.; Makarova, N. N.; Matukhina, E. V. Mesophase behavior and structure of mesophases in cyclolinear polyorganosiloxanes. In *Silicones and Silicone Modified Materials*; Clarson, S., Fitzgerald, J. J., Owen, M. J., Smith, S. D., Eds.; ACS Symposium Series 729; American Chemical Society: Washington, D.C., 2000; Chapter 6, pp 98−115.
(45) Fang, J.; Dennin, M.; Knobler, C. M.; Godovsky, Yu. K.; Makarova, N. N.; Yokoyama, H. *J. Phys. Chem. B*, **1997**, *101*, 3147.
(46) Buzin, A. I.; Sauter, E.; Godovsky, Yu. K.; Makarova, N. N.; Pechhold, W. *Colloid Polym. Sci.* **1998**, *276*, 1078.
(47) Buzin, A. I.; Sautter, E.; Godovsky, Yu. K.; Makarova, N. N.; Pechhold, W. *Russ. Polym. Sci.* **1998**, *A 40*, 43.
(48) Belousov, S. I.; Buzin, A. I.; Godovsky, Yu. K. *Russ. Polym. Sci.* **1999**, *B41*, 1687.
(49) Buzin, A. I.; Godovsky, Yu. K.; Makarova, N. N.; Fang, J.; Wang, X.; Knobler, C. M. *J. Phys. Chem. B* **1999**, *103*, 11372.
(50) Sautter, E. University of Ulm, Germany, private communication.
(51) Makarova, N. N.; Petrova, I. M.; Godovsky, Yu. K.; Zhdanov, A. A. Patent (Russia) N1126579, 1993.
(52) Makarova, N. N.; Godovsky, Yu. K.; Lavrukhin, B. D. *Russ. Polym. Sci.* **1995**, *A37*, 225−241.
(53) Makarova, N. N.; Lavrukhin, B. D. *Izv. Akad. Nauk SSR, Ser. Khim.* **1986**, 652.
(54) Makarova, N. N.; Godovsky, Yu. K. *Prog. Polym. Sci.* **1997**, *22*, 1001.
(55) Godovsky, Yu. K.; Makarova, N. N.; Kuzmin, N. N. *Makromol. Chem., Macromol. Symp.* **1989**, *26*, 91.
(56) Polistshuk, A. P.; Makarova, N. N.; Astapova, T. V. *Krystallografiya* **2002**, *47*, 863−868.

(57) Frahm, R.; Weigelt, J.; Meyer, G.; Materlik, G. *Rev. Sci. Instrum*. **1995**, *66* (2), 1677.
(58) Als-Nielsen, J.; Jacquemain, D.; Kjaer, K.; Leveiller, F.; Lahav, M.; Leiserowitz, L. *Phys. Rep*. **1994**, *246*, 251.
(59) Kjaer, K. *Physica B* **1994**, *198*, 100.
(60) Jensen, T. R.; Kjaer, K. In *Novel Methods to study Interfacial Layers, Studies in Interface Science*; Möbius, D., Miller, R., Eds.; Elsevier Science B.V.: New York, 2001; Vol. 11, pp 205−254.
(61) Vollhard, D.; Gehlert, U.; Siegel, S. *Colloids Surf. A* **1993**, *76*, 187.
(62) Wunderlich, B.; Chen, W. In *Liquid-Crystalline Polymer Systems*; Isaev, A. I., Thein Kyu, Cheng, S. Z. D., Eds.; ACS Symposium Series 632; American Chemical Society: Washington, D.C., 1996; pp 232−248.
(63) Jensen T. R.; Kjaer, K.; Brezesinski, G.; Ruiz-Garcia, J.; Möhwald, H.; Makarova, N. N.; Godovsky, Yu. K. *Macromolecules* **2003**, *36*, 7236−7243.
(64) Kampf, J. P.; Frank, C. W.; Malmstroem, E. E.; Hawker, C. J. *Science* **1999**, *283*, 1730.
(65) Als-Nielsen, J.; Kjaer, K. X-Ray reflectivity and diffraction studies of liquid surfaces and surfactant monolayers. In *Phase transitions in soft condensed matter. NATO Advanced Study Institute on phase transitions in soft condensed matter, Geilo, 4−14 Apr 1989*; Riste, T., Sherrington, D., Eds.; Plenum Press: New York, 1989; (NATO Advanced Science Institutes Series B: Physics, 211) pp 113−138.

MA049631U